RSC Advances

ROYAL SOCIETY OF CHEMISTRY

www.rsc.org/advances

RSC Advances

ARTICLE

Surface Defection Reduces Cytotoxicity of Zn(2-methylimidazole)$_2$ (ZIF-8) without Compromising its Drug Delivery Capacity

Received 11th November 2015,
Accepted 00th January 2016

DOI: 10.1039/x0xx00000x

www.rsc.org/

Emily Shearier [1, #], Peifu Cheng [2, #], Jiming Bao[3], Yun Hang Hu [2, *] and Feng Zhao [1, *]

Zn(2-methylimidazole)$_2$ (ZIF-8), as one of the important metal-organic framework (MOF) molecules, is a promising candidate for drug delivery due to its low-density structure, high surface area, and tunable frameworks. However, ZIF-8 exhibits a high cytotoxicity associated with its external hydrophobic surface, which significantly restricts its application in drug delivery and other biomedical applications. Commonly used chemical functionalization methods would convert the hydrophobic surface of ZIF-8 to hydrophilic, but the generated functional groups on its internal surface may reduce its pore sizes or even block its pores. Herein, a surface defection strategy was applied on the external surface of ZIF-8 to enhance its hydrophilicity without reducing or blocking the internal pores. In this approach, mechanical ball-milling was used to incur defects on the external surface of ZIF-8, leading to unsaturated Zn-sites and N-sites which subsequently bound H_2O molecules in an aqueous environment. Furthermore, hydroxyurea delivery and cell cytotoxicity of ZIF-8 with and without the external surface treatment were evaluated. It was found that 5-min ball milling turned over the hydrophobic–hydrophilic balance of ZIF-8, resulting in significantly higher cell viability without compromising its hydroxyurea loading and release capacity. Such a simple mechanical ball-milling followed by water-treatment provides a general technique for surface-modification of other MOF molecules, which will undoubtedly magnify their biomedical applications.

Introduction

Metal-organic frameworks (MOFs) are a new class of nanoporous materials that consist of metal clusters coordinated to organic linkers [1-8]. Due to their low-density structures, high surface areas, and tunable frameworks, MOFs have been widely used in the fields of gas storage, catalysis, optical and sensor technologies [9-12]. Moreover, MOFs are versatile, biodegradable, and contain hydrophilic–hydrophobic internal microenvironments that are compliant to host different molecules [13]. These unique properties offer MOFs great opportunity for sustained drug release applications [13-18].

Among the multiple types of MOF compounds, zeolitic imidazolate frameworks (ZIFs) are constructed with tetrahedral units formed by one bivalent metal M^{2+} cations (usually Zn^{2+}) and four imidazolate anions (Im-), analogous to SiO_2 tetrahedra in zeolites [4-6, 11, 12, 19-21]. While the imidazole is an essential group of the amino acid histidine, Zinc is the second most abundant transition metal in biology, and plays an important role in physiological systems. The special chemical components of ZIFs make them especially attractive as drug carriers. As a representative ZIF, Zn(2-methylimidazole)$_2$ (ZIF-8) possesses a sodalite zeolite-type structure with large pores (11.6 Å in diameter), which are connected by apertures (3.4 Å in diameter). Our previous publications have revealed that bivalent cations result in a structural collapse of ZIF-8, and even water causes a gradual change in ZIF-8 crystal structure [22, 23]. Because of the large pore size, high surface area, as well as its degradability in aqueous environment, ZIF-8 has attracted much attention for delivering both hydrophilic and hydrophobic drugs, including 5-fluorouracil [24], doxorubicin [25], and several other drugs [26].

Unfortunately, the cytotoxicity of ZIF-8 is relatively high because of its hydrophobic nature [27]. To reduce the cytotoxicity of ZIF-8 and increase the cell viability, the hydrophobic–hydrophilic balance of ZIF-8 has been adjusted via surface grafting, functionalization of its imidazolate linkers, and particle encapsulation in hydrogel spheres [27, 28]. However, these complex chemical processes not only functionalize the external surfaces of ZIF-8, but also bring changes to its internal surface, which inevitably reduce their pore size or even block the pores, and subsequently inhibit the diffusion of drug molecules into the pores. Thus, the ideal modification of ZIF-8 should only convert its external surface from hydrophobicity to hydrophilicity, without reducing or blocking its internal pores.

In this study, a surface defection strategy is designed to specifically target the external surface of ZIF-8 for its hydrophobic-hydrophilic conversion. A portion of Zn-N bonds on the external surface of ZIF-8 are attacked by a mechanical force, resulting in unsaturated Zn-

[a] Department of Biomedical Engineering, Michigan Technological University, Houghton, MI 49931.
[b] Department of Materials Science and Engineering, Michigan Technological University, Houghton, MI 49931.
[c] Department of Electrical & Computer Engineering, University of Houston, Houston TX 77204.
* Corresponding authors.
# Equal contribution.
Electronic Supplementary Information (ESI) available: [details of any supplementary information available should be included here]. See DOI: 10.1039/x0xx00000x

sites and N-sites, which in turn bind H_2O molecules in an aqueous environment. Since the mechanical force can be controlled to only marginally modify the external surface of ZIF-8, the internal pore structure and size will be well preserved to maintain its drug loading and release capacity. To realize this design, a simple ball-milling approach was used to generate mechanical force to break the Zn-N bonds on the external surface of ZIF-8 particles in a closed system. The drug delivery capability of ZIF-8 particles with and without defection was then evaluated by delivering a model drug, hydroxyurea, a small hydrophilic organic molecule that has been used in several serious diseases [29-34]. The cytotoxicity of ZIF-8, with and without defects, was also performed on human dermal fibroblasts (hDFs), a cell type commonly used for biomaterial cytotoxicity testing [35-37]. It was found that a simple 5-minute ball-milling turned ZIF-8 from hydrophobic to hydrophilic, and significantly improved its cell viability without compromising its drug carriage and release capacity.

Materials and Methods

Preparation of ZIF-8 Samples

ZIF-8 was purchased from Sigma-Aldrich (St. Louis, MO). ZIF-8 particles (600 mg) were placed inside a stainless steel container alongside three stainless steel milling balls. A SPEX 8000 Mixer/Mill was used to ball-mill the ZIF-8 for 5 min, 10 min, and 30 min at room temperature. The as-obtained samples were denoted as ZIF-8-5min, ZIF-8-10min, and ZIF-8-30min, respectively.

ZIF-8 Characterization

The X-ray diffraction (XRD) was performed on ZIF-8, both pristine and ball-milled, to detect their crystal structure. Samples with a volume of 0.2 cm^3 were placed in a Scintag XDS-2000 powder diffractometer at 45 kV and 35 mA for Cu Kα (λ=1.54062 Å) radiation, with a scan speed of 1^o/min and a step size of 0.03^o in 2θ. This analysis was performed under 1 atm at room temperature. Crystal size was further calculated by the Scherrer equation [23]:

$$\tau = \frac{K\lambda}{\beta cos\theta}$$

Where τ is the crystal size, K is the dimensionless shape factor, λ is the X-ray wavelength, β is the full width at half maximum (FWHM), and θ is the Bragg angle.

Surface areas of the pristine and defected ZIF-8 were measured using a Micromeritics ASAP 2000 sorptometer with nitrogen adsorption at liquid-nitrogen temperature (77 K). 0.1 g of each sample was tested. Before measurement, all samples were degassed at 200 ^oC for 12 hours to remove any guest molecules. Total surface areas were calculated by the Brunauer-Emmett-Teller (BET) model [38].

The morphologies of the pristine and defected ZIF-8 were determined by a Hitachi S-4700 field emission scanning electron microscope (FE-SEM) (Hitachi High Technologies, Tokyo, Japan) with an acceleration voltage of 5 kV and 12 mm working distance. Before taking images, the samples were coated by carbon.

Fourier transform infrared spectroscopy (FT-IR) spectra of both pristine and ball-milled ZIF-8 particles were obtained by using a Perkin Elmer Spectrum One spectrometer (Shelton, CT). All samples were dried at 120 ^oC under vacuum for 12 hours before measurement.

Dynamic light scattering (DLS) was used to record particle size distributions of ZIF-8 and defected ZIF-8 by Brookhaven BI-200SM multiangle laser light scattering system (Brookhaven Instruments, Holtsville, NY). These samples were exposed to ultrasonic for 15 minutes and then allowed to stand for 3 days. The parameters used were 15 mW laser power, 90^o collection angle, 25 ^oC surrounding temperature, and 400 aperture. Three measurements were collected for each sample. Particle size distribution was shown in particle number and particle volume.

Drug Loading and Release

For drug loading, 10 mg of ZIF-8 samples were immersed in 100 mL of phosphate-buffered saline (PBS) under stirring at 37 ^oC for 30 min. After that, 30 mg of hydroxyurea (Sigma-Aldrich) was added into the suspension. Every 12 h, the suspension was filtered to obtain a clear hydroxyurea solution for UV-Vis measurement. The solid residue (ZIF-8 loaded with hydroxyurea) was diluted in 100 mL of PBS to re-suspend the material and continue the test.

The UV-Vis was used to measure the hydroxyurea concentration in PBS during drug adsorption and release processes. UV-Vis spectra were recorded at room temperature with a UV-Vis spectrometer (Shimadzu UV-2400) in the range of 200–800 nm under absorbance mode (Supplementary Figure S1). 3.5 mL of particle suspension was used for each sample type. PBS was used as the background standard.

ZIF-8 Supernatant Cytotoxicity

The supernatant cytotoxicity was first used to determine if any substances from the ZIF particles leached out during an incubation period in an aqueous solution were harmful to cells. This helped establish a starting point for determining if a substance was cytotoxic. To obtain ZIF-8 supernatant, 0.2 g of the pristine ZIF-8 was placed in 10 mL PBS for 72 h at room temperature with stirring. hDFs (ATCC, Manasass, VA) were cultured in Dulbecco's Modified Eagle Medium (DMEM) supplemented with 20% fetal bovine serum (FBS), 20% Ham F12, 500 μM sodium ascorbate and 1% penicillin/streptomycin (Life Technologies, Rockville, MD). The hDFs were seeded at a density of 4,500 cells/cm^2 in a 96 well plate. ZIF-8 supernatant was added in five quantities to 2 mL media at 10, 20, 50, 100, and 200 μL. 6 samples per data point were used for each level. The cells were then cultured for 24 hours. Cell viability was analysed using an XTT assay (ATCC). Cells were grown on glass coverslips and exposed to the same levels of supernatant as XTT tests, cultured for 24 hours, and visualized using fluorescent microscopy. 6 samples were used for each condition. hDFs were fixed, blocked, and incubated with Rodamin Phalloidin (Life Technologies) for 1 hour followed by washing and 4', 6-diamidino-2-phenylindole (DAPI, Sigma-Aldrich) solution to stain the cell nuclei. Images were visualized under an Olympus BX-51 fluorescence microscope. At least 6 fields of views were imaged for each sample.

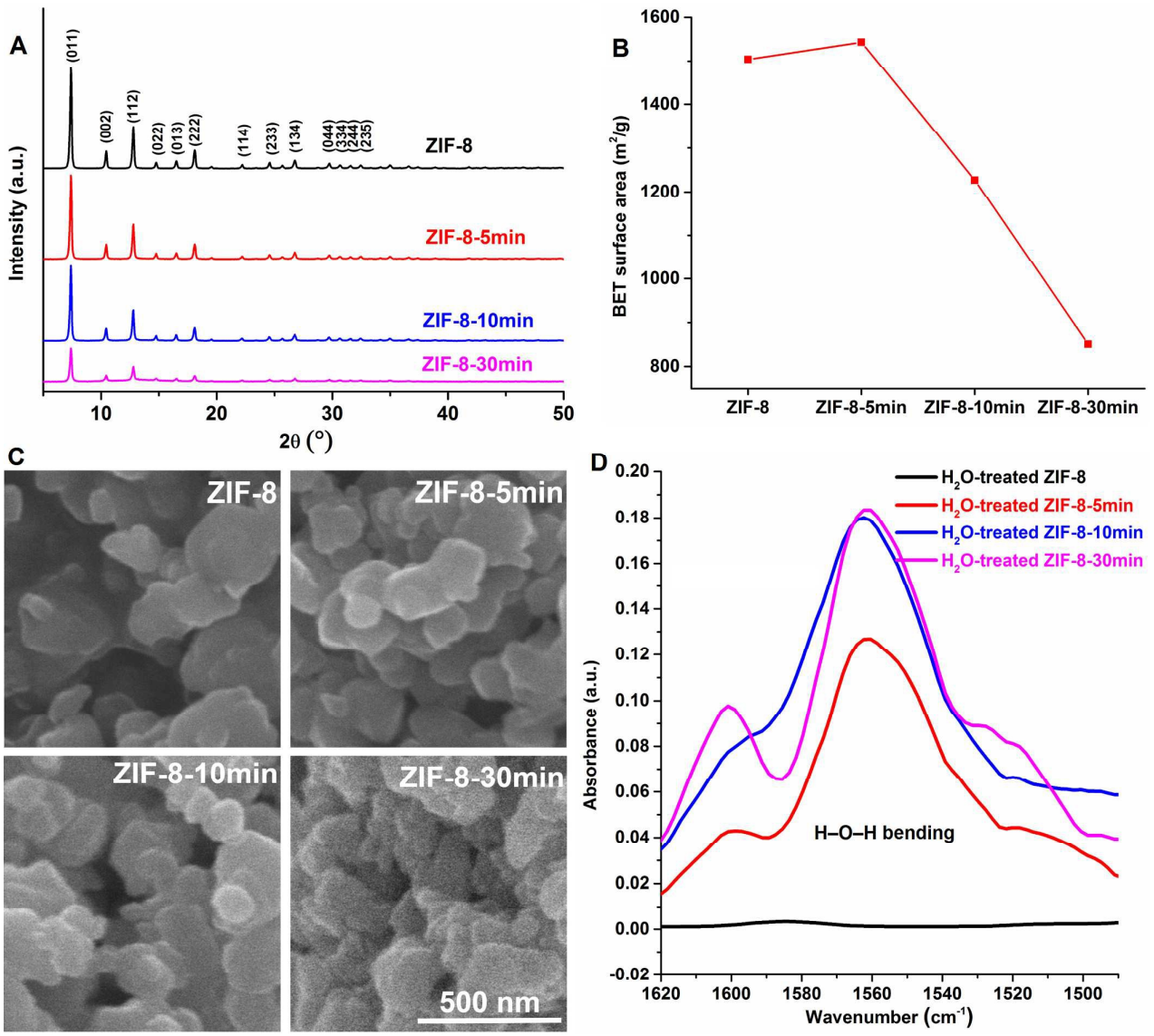

Figure 1 Characterization of ZIF-8, ZIF-8-5min, ZIF-8-10min, and ZIF-8-30min powders. (A) XRD patterns, (B) BET surface areas, (C) FE-SEM morphology images, and (D) FT-IR subtraction spectra of H_2O-bound samples in phosphate-buffered saline (PBS). The FT-IR subtraction spectra were obtained by subtracting the IR spectrum of pristine ZIF-8 from those of H_2O-bound ZIF-8, ZIF-8-5min, ZIF-8-10min, and ZIF-8-30min.

In order to measure the Zn^{2+} to which the cells were exposed, inductively coupled plasma optical emission spectrometry (ICP-OES) was performed on supernatant obtained from pristine samples, as well as 5, 10, and 30 min ground samples, prepared in the same manner as described above for supernatant, using a Perkin-Elmer 7000 DV (Waltham, MA). 5 mL of each solution was tested. The ICP-OES detection limit for Zn^{2+} was 6 ppb. 6 samples were used for each condition, and at least 6 fields of views were imaged for each sample.

ZIF-8 Particle Cytotoxicity

ZIF-8 particles were suspended in PBS as described above, with both pristine and ground particles analysed. hDF cells were cultured using the same media and at the same density for 48 hours in a 96-well plate to establish a layer of cells to be insulted with particles. The particle suspension was added to the media in quantities ranging from 1 to 200 µL to 2 mL of media. This corresponded to 20 to 1000 µg of ZIF-8 powder added to each sample. Cells were cultured for 24 hours after exposure. Cell viability was once again determined using an XTT assay, with 6 samples per data point used for each level. Lethal dose 50% (LD_{50}), the amount of substance that kills 50% of the test sample, was thus determined. Similar culture conditions were used for fluorescent staining, with the cells seeded on glass coverslips for 48 hours, and then exposed to the same levels of particles for 24 hours. Cells were then visualized using the fluorescent microscopy technique described above. At least 6 fields of views were imaged for each sample.

Statistical Methods

Quoted errors and error bars correspond to sample standard error. Beers' approach to the propagation of random errors was used to calculate overall standard errors for the XTT assay that took into account random error in measurements from the experimental group and background (blank) samples. Student's t-test (Microsoft

Excel) was used for comparisons, and statistical significance was accepted at $P < 0.01$.

Results

ZIF-8 Characterization

Powder XRD patterns were measured to evaluate the effect of defects on the crystal structure of ZIF-8. As shown in Figure 1A, the XRD pattern of ZIF-8 was consistent with the results reported in literature [24, 26]. After ball milling, the intensities of all diffraction peaks decreased, indicating the crystal structure of ZIF-8 was damaged while defects were generated gradually. This was supported by the change of average crystal sizes (calculated by the Scherrer equation [23]) of ZIF-8, which were 51.22 nm (ZIF-8), 50.11 nm (ZIF-8-5min), 49.46 nm (ZIF-8-10min), and 43.75 nm (ZIF-8-30min). The continuous decrease in crystal size was attributed to the chemical bond breakage on the external surface of ZIF-8 at the beginning of ball milling, followed by the structural damage over time. This was further supported by the results of BET surface areas (Figure 1B) and particle size distribution (Supplementary Figure S3). The BET surface area increased slightly in the first 5 minutes and then decreased sharply with increasing ball-milling time (Figure 1B). The particle size distribution showed that the particle size had a tighter distribution (ZIF-8-5min) and then the distribution became wider (ZIF-8-10min and ZIF-8-30min) with increased time, while the average particle size calculated from volume also showed a decrease in the first 5-min and then increased in the 10 min and 30 min ball milling samples (Figure S3). In addition, no significance difference was observed in the morphology of pristine and defected ZIF-8 samples as observed by FE-SEM (Figure 1c).

The hydrophobicity/hydrophilicity of pristine and defected ZIF-8 samples was investigated by using FT-IR spectrometry. After treated in PBS, which was used as drug loading medium, the H-O-H bending groups in the range of 1620 to 1490 cm^{-1} appeared in the FT-IR spectra of all the defected ZIF-8 samples, indicating H_2O was bound in these particles (Figure 1D). The bands of pristine ZIF-8 were consistent with our previous publication [23]. The FT-IR subtraction spectra of defected ZIF-8 were calculated by subtracting the IR spectrum of ZIF-8 from those of defected ZIF-8 samples. With the increase of defects, the content of H-O-H bending groups in ZIF-8 firstly increased from 75.7% (ZIF-8-5min) to 100% (ZIF-8-10min) and then to 107.2% (ZIF-8-30min), suggesting that the hydrophilicity of ZIF-8 firstly increased and then remained almost unchanged after 10 min ball-milling.

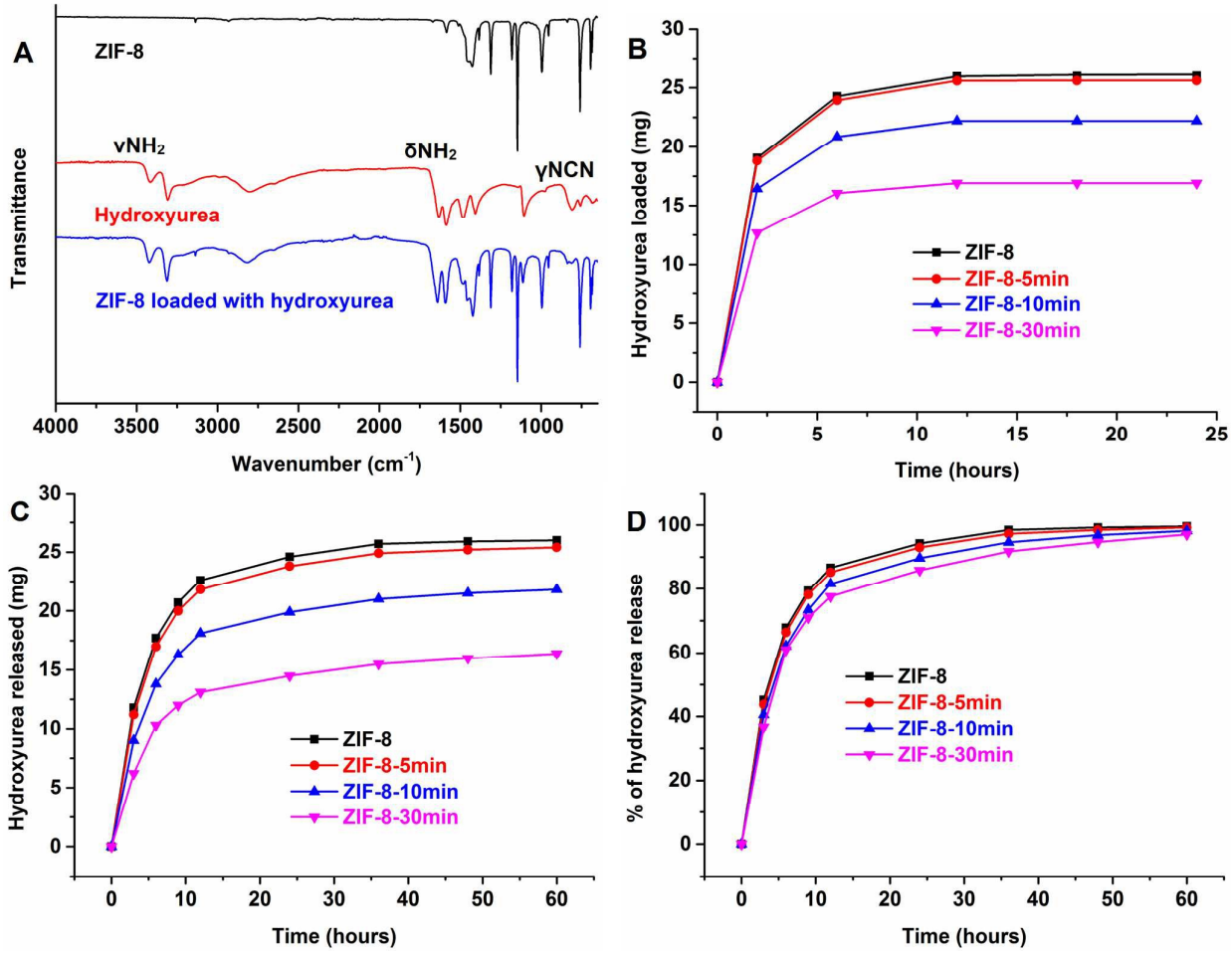

Figure 2 Drug loading and release profile in ZIF-8, ZIF-8-5min, ZIF-8-10min, and ZIF-8-30min powders. (A) FT-IR spectra of ZIF-8, hydroxyurea, and hydroxyurea loaded ZIF-8. (B) Adsorption profile of hydroxyurea over 24h. (C) Release profile of hydroxyurea over 60h. (D) Percentage of hydroxyurea released at different times.

ZIF-8 Uptake and Release of Drug Hydroxyurea

FT-IR spectrometry was used to obtain the absorption features of pristine and defected ZIF-8 samples before and after drug adsorption. After hydroxyurea adsorption, all the ZIF-8 samples loaded with hydroxyurea displayed peaks of H–N–H stretching (3415cm^{-1}), H–N–H bending (1632 cm^{-1}), and N–C–N bending (807 cm^{-1}), which are typical absorption features of hydroxyurea (Figure 2A) [39]. These spectra indicated that hydroxyurea had been incorporated in the particles. UV-Vis spectra of filtrates at different time points were collected to evaluate the concentration change of hydroxyurea in filtrates during the adsorption and desorption processes. Figure 2B showed that the hydroxyurea loaded in all samples gradually increased and reached a maximal amount around 12 h, while the cumulative amounts of hydroxyurea adsorbed in different samples (26.1 mg, 25.6 mg, 22.2 mg, and 16.9 mg for pristine, ZIF-8-5min, ZIF-8-10min, and ZIF-8-30min samples, respectively) decreased with the increase of defects (Figure 2B). Furthermore, the ZIF-8-5min samples displayed exactly the same trend of drug loading as the pristine samples over the entire 60 h of drug absorption period. There were no significant differences between the amounts of loaded drugs for all time points. The drug release curves of ZIF-8-5min samples almost overlapped with that of the pristine samples, both in total amount (Figure 2C) and release rate (Figure 2D) over 60h. Whereas the ZIF-8-10min and ZIF-8-30min samples exhibited significantly lower amounts of hydroxyurea released (Figure 2D) and a slightly slower release rate during the 60 h period (Figure 2D).

Supernatant Cytotoxicity Tests

hDFs were exposed to supernatant extracted from pristine and 5, 10, and 30 min defected ZIF-8 samples (3 samples each), with only pristine particles shown, to evaluate their cell viability using an XTT assay. The cell viability as a percentage of the PBS control can be seen in Figure 3A. The two dashed lines on the graph represent the control upper and lower standard deviation. For each condition, as high as 200 µL of supernatant was added in each cell culture sample, the cell viability was not different from the control samples for the pristine supernatant, with similar values exhibited in all

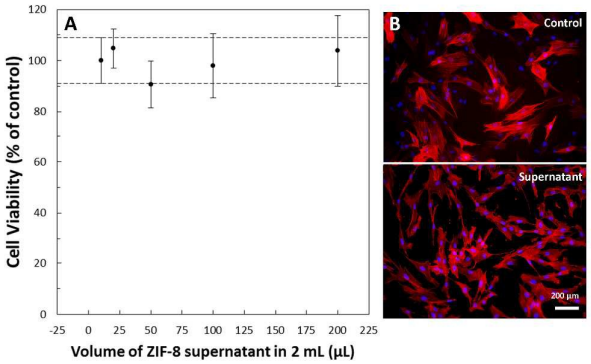

Figure 3 The cytotoxicity assay for supernatant extracted from ZIF-8 particles. (A) Cell viability of hDFs cultured with supplementary ZIF-8 supernatant at different concentrations. Even at the highest concentration, the cell viability was not significantly different from the PBS control. Cell viability was measured using an XTT assay. (B) Cell morphology of hDFs after exposure to 200 µL of ZIF-8 supernatant and control. Red: F-actin; Blue: cell nuclei. Scale bar: 200 µm.

defected ZIF-8 samples (data not shown). The supernatant containing free Zn^{2+} did not induce cytotoxicity in the hDFs, with the levels of Zn^{2+} shown in Supplementary Figure S2 as determined by ICP-OES. Zn levels shown in Figure S2 ranged from 300 to 600 ppm in the PBS supernatant, and this was diluted 20X leading to levels of 15 to 30 ppm. PBS itself contained 35 ppm Zn, similar to the Zn content in cell culture media. Therefore, the Zn^{2+} released from the ZIF-8 particles to the supernatant was minimal.

The cell morphology was observed by staining F-actin (a cytoskeletal protein) and cell nuclei. For all investigated conditions, the hDFs displayed good structural integrity and appeared healthy. This was shown in Figure 3B, after the cells were exposed to 200 µL supernatant for 24 h.

Direct Contact Particle Cytotoxicity

After it was demonstrated that hDF cells were not affected by

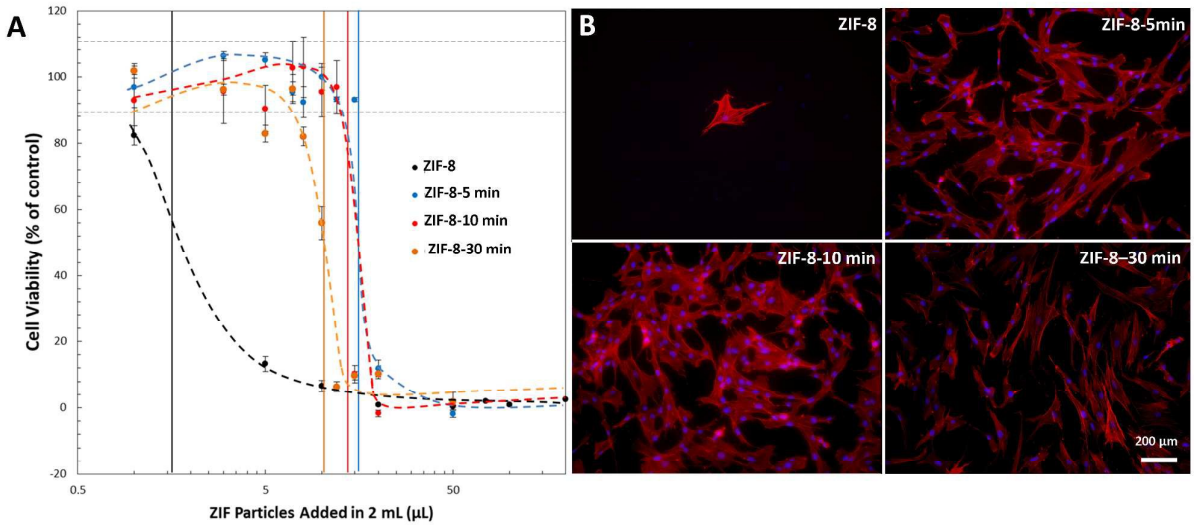

Figure 4 The direct contact cytotoxicity assay for ZIF-8, ZIF-8-5min, ZIF-8-10min, and ZIF-8-30min powders. (A) Cell viability of hDFs cultured with supplementary particle suspensions at different concentration. LD50 is represented by lines the same color corresponding to the condition. Ground 5, 10, and 30 min had no significant difference between LD50 values. Trend lines (dashed lines) were added to guide the eye. (B) Cell morphology of hDFs after exposure to 5 µL of different particle suspension. Red: F-actin; Blue: cell nuclei. Scale bar: 200 µm.

supernatant taken from ZIF-8 particles and consequential exposure to Zn^{2+}, direct contact was investigated. In initial experiments particle suspension of pristine ZIF-8 was added to samples. This was shown to be extremely cytotoxic, with very few living cells remaining after exposure.

Due to the fact that pristine particles exhibited a very poor interaction with the cells, processed particles were of interest. The particles were evaluated at the same levels as the pristine after 5, 10, and 30 min ball milling. This processing resulted in a dramatic increase in viability of hDF cells, as shown in Figure 4A. The LD_{50} for pristine particles was 40 µg of suspended particles per sample, whereas the ground particles' LD_{50} ranged from 180 to 240 µg of suspended particles per sample and were not significantly different among the ball-milling times. The pristine and all ball milling samples were then visualized using fluorescent microscopy and stained for F-actin (red) and cell nuclei (blue) after exposure to 100 µg of suspended particles per sample and are shown in Figure 4B. Good cell morphology and viability was seen in all ball-milled groups. This stands in stark contrast to the pristine material, which killed almost all cells present in the environment.

Discussion

The drug adsorption and desorption was dominated by the interaction between the drug molecules and the drug carrier. During the drug adsorption process, the host-guest interaction controlled the drug diffusion through the porous structure [4, 13]. The adsorption of hydroxyurea on pristine ZIF-8 was mainly controlled by the van der Waals forces generated physisorption. Since the most vulnerable bond in a MOF molecule was the one between an inorganic cluster and an organic ligand [2, 6, 9, 23, 40], the Zn-N bonds were broken after ball-milling, leading to unsaturated Zn-sites and N-sites. When placed in PBS for drug adsorption, these unsaturated Zn-sites and N-sites of defected ZIF-8 were re-saturated by H_2O molecules [9], turning the hydrophobic particles external surface into a hydrophilic one (Scheme 1). Our previous density functional theory (DFT) calculation has proven that H_2O molecules are bound to unsaturated Zn-sites of ZIF-8 through their oxygen atoms with binding energy of 80.5 kJ/moL, and the hydrogen atoms of H_2O molecules are bound to the unsaturated N-sites of ZIF-8 with binding energy of 31.7 kJ/mol. The two energies are both much higher than the binding energy of physisorption (usually less than 10 kJ/moL), thus the unsaturated sites were preferentially re-saturated by H_2O in PBS [23].

The ZIF-8-5min particles were ground smaller (Supplementary Figure S3), leading to a slightly increased surface area compared with their pristine counterparts (Figure 1B). The particles were also marginally damaged, turning their exterior surfaces hydrophilic (Figure 1D). However, the internal surfaces of ZIF-8 crystals were well preserved. The diffusion mechanism of hydroxyurea into and out of the pores of ZIF-8 was thus not affected by the external surface changes of the particles. Hence, the hydroxyurea loading and release capacity was only minimally compromised (Figure 2B and 2C). Whereas the long time ball milling (10-30 min) severely damaged the crystal as well as pore structure of ZIF-8, which explained the dramatically decreased surface area (Figure 1B) and the significantly lowered amount of loaded drugs (Figure 2B).

The biocompatibility of ZIF is important for its drug delivery applications. ZIF particles are of particular interest due to their

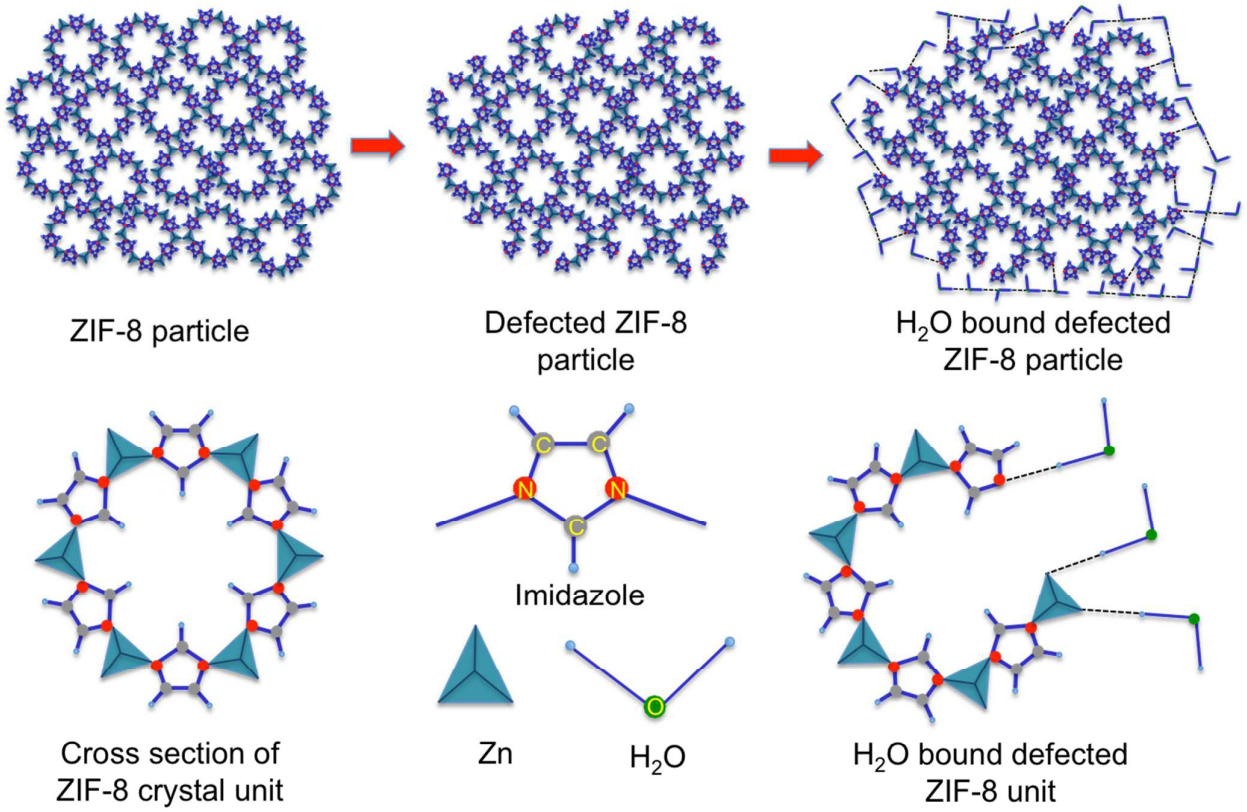

Scheme 1. Schematic illustration of the proposed mechanism of the introduction and defects and breakage of bonds, leading to unsaturated Zn-sites and N-sites. These bonds, in turn, will bind H_2O in aqueous environment.

ability to release their molecules using a pH trigger [24]. hDFs were cultured to determine the cytotoxic effect of ZIF-8 particles, with supernatant tests to determine chemical interactions and direct contact to investigate both chemical and physical interactions. Three variables in the environment might influence the cell viability: 1. Zn^{2+} ions released from the particles; 2. ZIF-8 particle size and morphology; 3. the hydrophobic–hydrophilic balance of the external surface of ZIF-8. The Zn^{2+} ions in the environment appeared to be of no concern, as their low concentration was comparable to that of the cell culture media, and they were also buffered by proteins existing in cell culture media [41]. The reasoning was further proven by hDFs cultured in the particle supernatant, which showed no decrease of cell viability (Figure 3). The particle morphology was not a factor either, because no significance change was observed in the particle morphology before and after ball-milling. As to the particle size, after ball-milling, the ZIF-8 particle distribution ranged from 185 μm (ground 10 min) to 7718 μm (ground 5 min), which was even more broader than the pristine ZIF-8 particles (323 μm to 2291 μm). This result indicated that the particle size within this range was not a major factor that affected the cytotoxicity, because pristine ZIF-8 particles exhibited unexpectedly high levels of cytotoxicity, whereas all the defected particles had greatly improved viability ratios (Figure 4).

The lowered cytotoxicity was thus attributed to the enhanced hydrophilicity of ZIF-8 after ball-milling. Cytotoxicity was reported to strongly depend on the hydrophobic–hydrophilic balance of MOFs, and hydrophilic groups showed a low cytotoxicity [27]. ZIF-8, which was stable in PBS, was hydrophobic which may lead to relative high cytotoxicity, as had been shown in several studies [42, 43] and our results (Figure 4). The ball milling, independent of milling time from 5 to 30 minutes, turned all the defected samples to hydrophilic, giving rise to significantly improved cell viability in all the direct contact cell cultures (Figure 4).

Conclusions

In summary, a surface defection approach, as simple as 5-min ball-milling, was applied to break a portion of Zn-N bonds on the external surface of ZIF-8. The resulted unsaturated Zn-sites and N-sites bound H_2O molecules in an aqueous environment, converting the external surface of the ZIF-8 into hydrophilic while preserving the structure and chemistry of internal pores. The hydrophobic-hydrophilic conversion of the external surface of ZIF-8 significantly increased cells' tolerance for the particles without compromising their drug loading and delivery capacity. This simple surface defection strategy could be applied to other MOF molecules. Although different MOF molecules have varying structure stabilities, the modification method could be correspondingly adjusted by optimizing the ball-milling time and speed, and by tuning the ball size. This external surface defection strategy will undoubtedly enhance the drug delivery as well as other biomedical applications of MOF molecules.

Acknowledgements

This study was supported by the National Institutes of Health (1R15HL115521-01A1) and the Research Excellence Fund-Research Seed Grant (REF-RS) from Michigan Technological University to F.Z. This work was also supported by the U.S. National Science Foundation (NSF-CBET-0929207) to Y.H.

References

1. S. S. Kaye, A. Dailly, O. M. Yaghi and J. R. Long, *J Amer Chem Soc,* 2007, **129**, 14176-14177.
2. S. Noro, S. Kitagawa, M. Kondo and K. Seki, *Angew Chem Int Ed Engl*, 2000, **39**, 2081-2084.
3. J. S. Seo, D. Whang, H. Lee, S. I. Jun, J. Oh, Y. J. Jeon and K. Kim, *Nature*, 2000, **404**, 982-986.
4. H. Hayashi, A. P. Cote, H. Furukawa, M. O'Keeffe and O. M. Yaghi, *Nat Mater*, 2007, **6**, 501-506.
5. B. Wang, A. P. Cote, H. Furukawa, M. O'Keeffe and O. M. Yaghi, *Nature*, 2008, **453**, 207-211.
6. R. Banerjee, A. Phan, C. Knobler, H. Furukawa, M. O'Keeffe and O. M. Yaghi, *Science*, 2008, **319**, 939-943.
7. Z. Chang, D. H. Yang, J. Xu, T. L. Hu and X. H. Bu, *Adv Mater* 2015, **27**, 5432-5441.
8. H. Wang, J. Xu, D.-S. Zhang, Q. Chen, R.-M. Wen, Z. Chang and X. H. Bu, *Angew Chem Int Ed Engl*, 2015, **54**, 5966-5970.
9. Y. H. Hu and L. Zhang, *Adv Mater*, 2010, **22**, E117-E130.
10. B. Li, Y. Zhang, D. Ma, T. Ma, Z. Shi and S. Ma, *J Amer Chem Soc*, 2014, **136**, 1202-1205.
11. X. C. Huang, Y. Y. Lin, J. P. Zhang and X. M. Chen, *Angew Chem Int Ed Engl*, 2006, **45**, 1557-1559.
12. H. Wu, W. Zhou and T. Yildirim, *J Amer Chem Soc*, 2007, **129**, 5314-5315.
13. A. C. McKinlay, R. E. Morris, P. Horcajada, G. Ferey, R. Gref, P. Couvreur and C. Serre, *Angew Chem Int Ed Engl*, 2010, **49**, 6260-6226.
14. C. Y. Sun, C. Qin, C. Wang, Z. Su, S. Wang, X. L. Wang, G. S. Yang, K. Z. Shao, Y. Lan and E. Wang, *Adv Mater*, 2011, **23**, 5629-5632.
15. P. Horcajada, C. Serre, M. Vallet-Regi, M. Sebban, F. Taulelle and G. Ferey, *Angew Chem* 2006, **118**, 6120-6124.
16. C. He, K. Lu, D. Liu and W. Lin, *J Amer Chem Soc*, 2014, **136**, 5181-5184.
17. P. Horcajada, T. Chalati, C. Serre, B. Gillet, C. Sebrie, T. Baati, J. F. Eubank, D. Heurtaux, P. Clayette, C. Kreuz, J. S. Chang, Y. K. Hwang, V. Marsaud, P. N. Bories, L. Cynober, S. Gil, G. Ferey, P. Couvreur and R. Gref, *Nat Mater*, 2010, **9**, 172-178.
18. H. Wang, T. L. Hu, R. M. Wen, Q. Wang and X. H. Bu, *J Mater Chem B*, 2013, **1**, 3879-3882.
19. K. S. Park, Z. Ni, A. P. Cote, J. Y. Choi, R. Huang, F. J. Uribe-Romo, H. K. Chae, M. O'Keeffe and O. M. Yaghi, *Proc Natl Acad Sci USA,* 2006, **103**, 10186-10191.
20. D. J. Collins and H. Zhou, *J Mater Chem*, 2007, **17**, 3154-3160.
21. J. Perez-Pellitero, H. Amrouche, F. R. Siperstein, G. Pirngruber, C. Nieto-Draghi, G. Chaplais, A. Simon-Masseron, D. Bazer-Bachi, D. Peralta and N. Bats, *Chem Eur J*, 2010, **16**, 1560-1571.
22. L. Zhang and Y. H. Hu, *J Phys Chem C*, 2011, **115**, 7967-7971.

23. P. Cheng and Y. H. Hu, *J Phys Chem C*, 2014, **118**, 21866-21872.
24. C. Y. Sun, C. Qin, X. L. Wang, G. S. Yang, K. Z. Shao, Y. Q. Lan, Z. M. Su, P. Huang, C. G. Wang and E. B. Wang, *Dalton Trans*, 2012, **41**, 6906-6909.
25. I. B. Vasconcelos, T. G. d. Silva, G. C. G. Militão, T. A. Soares, N. M. Rodrigues, M. O. Rodrigues, N. B. d. Costa, R. O. Freire and S. A. Junior, *RSC Adv*, 2012, **2**, 9437.
26. J. Zhuang, C. H. Kuo, L. Y. Chou, D. Y. Liu, E. Weerapana and C. K. Tsung, *ACS Nano*, 2014, **8**, 2812-2819.
27. C. Tamames-Tabar, D. Cunha, E. Imbuluzqueta, F. Ragon, C. Serre, M. J. Blanco-Prieto and P. Horcajada, *J Mater Chem B*, 2014, **2**, 262.
28. A. U. Ortiz, A. P. Freitas, A. Boutin, A. H. Fuchs and F.-X. Coudert, *Phys Chem Chem Phys*, 2014, **16**, 9940-9949.
29. C. N. Harrison, P. J. Campbell, G. Buck, K. Wheatley, C. L. East, D. Bareford, B. S. Wilkins, J. D. van der Walt, J. T. Reilly, A. P. Grigg, P. Revell, B. E. Woodcock and A. R. Green, *New Eng J Med*, 2005, **353**, 33-45.
30. S. Lanzkron, J. J. Strouse, R. Wilson, M. C. Beach, C. Haywood, H. Park, C. Witkop, E. B. Bass and J. B. Segal, *Ann Itern Med*, 2008, **148**, 939-955.
31. I. Frank, R. J. Bosch, S. Fiscus, F. Valetine, C. Flexner, Y. Segal, P. Ruan, R. Gulick, K. Wood, S. Estep, L. Fox, T. Nevin, M. Stevens and J. J. J. Eron, *AIDS Res Hum Retroviruses*, 2004, **20**, 916-926.
32. M. H. Rustin, *Br J Dermatol*, 2012, **167**, 3-11.
33. L. Escribano, I. Alvarez-Twose, L. Sanchez-Munoz, A. Garcia-Montero, R. Nunez, J. Almeida, M. Jara-Acevedo, C. Teodosio, M. Garcia-Cosio, C. Bellas and A. Orfao, *J Allerg and Clin Immuno*, 2009, **124**.
34. K. Dalziel, A. Round, K. Stein, R. Garside and A. Price, *Health Tech Asses* 2004, **8**, iii, 1-120.
35. C. M. Sayes, F. Liang, J. L. Hudson, J. Mendez, W. Guo, J. M. Beach, V. C. Moore, C. D. Doyle, J. L. West and W. E. Billups, *Toxicol Lett.*, 2006, **161**, 135-142.
36. M. Cooper, J. Laxer and J. Hansbrough, *J Trauma Acute Care Surg*, 1991, **31**, 775-784.
37. E. Hidalgo and C. Domınguez, *Toxicol Lett.*, 1998, **98**, 169-179.
38. S. Brunauer, P. H. Emmett and E. Teller, *J Amer Chem Soc*, 1938, **60**, 309-319.
39. M. Saldyka, *Phys Chem Chem Phys*, 2010, **12**, 15111-15118.
40. N. L. Rosi, J. Eckert, M. Eddaoudi, D. T. Vodak, J. Kim, M. O'Keeffe and O. M. Yaghi, *Science*, 2010, **300**, 1127-1129.
41. J. Raaflaub, *Applications of metal buffers and metal indicators in biochemistry*, John Wiley & Sons, Inc., Hoboken, NJ, 1956.
42. H. Vihola, A. Laukkanen, L. Valtola, H. Tenhu and J. Hirvonen, *Biomaterials*, 2005, **26**, 3055-3064.
43. H. Yin, P. S. Casey, M. J. McCall and M. Fenech, *Langmuir*, 2010, **26**, 15399-15408.